HIGH RESOLUTION DIGITAL SURFACE MODEL FOR PRODUCTION OF AIRPORT OBSTRUCTION CHARTS USING SPACEBORNE SAR SENSORS[1]

Henrique Oliveira[(1)], Marco Rodrigues[(1)], Andrea Radius[(2)]

[(1)]Escola Superior de Tecnologia e Gestão – Instituto Politécnico de Beja (ESTIG-IPB, Portugal)
Email : hjmo@lx.it.pt, marcoalexrodrigue@gmail.com
[(2)]Edisoft, Empresa de Serviços e Desenvolvimento de Software (Portugal), Email:andrea.radius@edisoft.pt

ABSTRACT

Airport Obstruction Charts (AOCs) are graphical representations of natural or man-made obstructions (its locations and heights) around airfields, according to International Civil Aviation Organization (ICAO) Annexes 4, 14 and 15. One of the most important types of data used in AOCs production/update tasks is a Digital Surface Model (first reflective surface) of the surveyed area.

The development of advanced remote sensing technologies provide the available tools for obstruction data acquisition, while Geographic Information Systems (GIS) present the perfect platform for storing and analyzing this type of data, enabling the production of digital ACOs, greatly contributing to the increase of the situational awareness of pilots and enhancing the air navigation safety level [1].

Data acquisition corresponding to the first reflective surface can be obtained through the use of Airborne Laser-Scanning and Light Detection and Ranging (ALS/LIDAR) or Spaceborne SAR Systems. The need of surveying broad areas, like the entire territory of a state, shows that Spaceborne SAR systems are the most adequate in economic and feasibility terms of the process, to perform the monitoring and producing a high resolution Digital Surface Model (DSM).

The high resolution DSM generation depends on many factors: the available data set, the used technique and the setting parameters. To increase the precision and obtain high resolution products, two techniques are available using a stack of data: the PS (Permanent Scatterers) technique [2], that uses large stack of data to identify many stable and coherent targets through multi-temporal analysis, removing the atmospheric contribution and to minimize the estimation errors, and the Small Baseline Subset (SBAS) technique ([3],[4]), that relies on the use of small baseline SAR interferograms and on the application of the so called singular value decomposition (SVD) method, in order to link independent SAR acquisition data sets, separated by large baselines, thus increasing the number of data used for the analysis.

1. SBAS PROCESSING FOR DSM GENERATION OF FARO'S AREA

To generate high resolution DEM of the Faro's test Area (south of Portugal) with the available datasets, the technique of Small BAseline Subsets (SBAS) was modified.

In fact, this technique was developed originally to generate deformation maps with differential interferometry (DINSAR). However, in our case, this technique was generalized to find the solution in case of across track interferometry (INSAR), in order to cope with the lack of images available to perform Persistent Scatterers, as originally intended.

The SBAS algorithm for DINSAR relies on the use of small baseline SAR interferograms and on the application of the so called singular value decomposition (SVD) method, in order to link independent SAR acquisition data sets, separated by large baselines, thus increasing the number of data used for the analysis. In our processing chain we selected relatively big baselines (between the 15% and 65% of the critical baseline) and used the same inversion scheme to retrieve a robust solution for the DEM, using all the good quality interferograms.

Two datasets of Envisat were available: 13 images in ascending orbit and 15 in descending orbit.

The SBAS processing was computed for each dataset independently.

The experience suggested than the best result was obtained with the Envisat ascending dataset, acquired at night in local time, because it shows less of such phase disturbance; the Envisat descending dataset, acquiring during the day, shows the impact of the atmospheric artefacts, generating some low quality interferograms.

After the selection of the candidate images which were compliant with the requirements of spatial and temporal baseline (the maximum allowed temporal baseline was selected to 480 days), the low-quality interferograms were excluded by the SBAS processing. Moreover, the so called unwrapping islands (closed areas for which the

[1] This research work is co-funded by the European Space Agency through the ITI TYPE C INICIATIVE: ESTEC Contract Nº. 22722/09/NLCBi, where EDISOFT (http://www.edisoft.pt) is the developer entity, ESTIG-IPB (www.ipbeja.pt) is the inventor entity and ANA Aeroportos de Portugal S.A. (http://www.ana.pt) is the costumer entity.

unwrapping algorithm was not able to well unwrap the phase) were manually removed.
The remaining modified unwrapped phase was used in SBAS processing to produce two high resolution DSMs (one for ascending dataset and one for descending dataset, shown respectively in fig. 1 and 2).

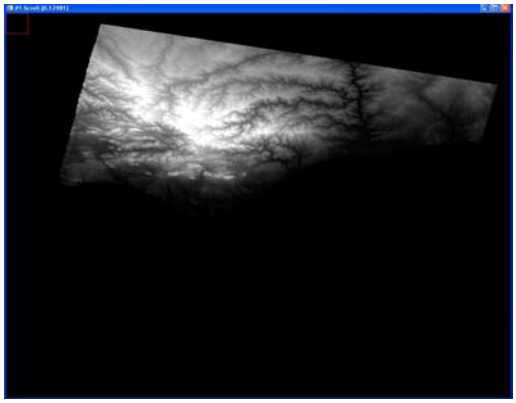

Figure 1. DSM generated by ascending dataset

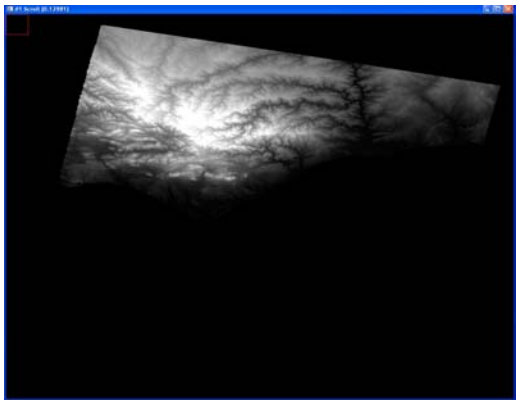

Figure 2. DSM generated by descending dataset

Finally, the two DSMs were summed to produce the final DSM (fig. 3). Note that the sum was weighted by coherence.
In according with ICAO requirements, the EGM-96 geoid of the Faro's test area was subtracted.

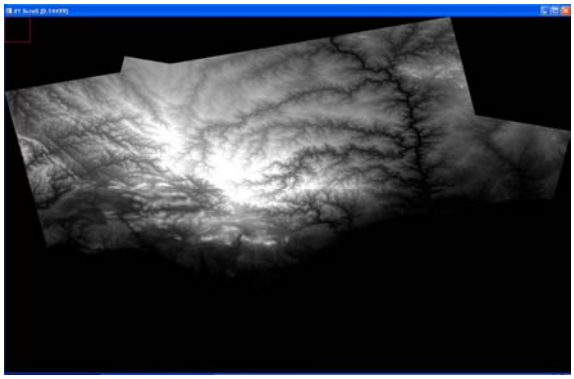

Figure 3. Final generated DSM

2. ATMOSPHERIC CONTRIBUTION REMOVAL

The atmospheric contribution was removed after the SBAS processing for each DEM.
Assuming that the atmosphere has high spatial correlation with low frequency, to remove this contribution the spatial low-pass filter was used.
To remove the contribute of the atmosphere, the low frequencies of the obtained high resolution DEM are substituted by the low frequencies of the reference DEM (SRTM) which, presumably, does not have atmospheric contributions.
For our processing, we used spatial filtering through Wavelet DEM Combination. The decomposition through the Wavelet transform is used to separate the low frequencies, as shown in fig.4.

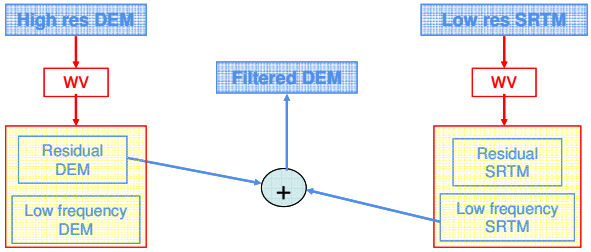

Figure 4. Wavelet scheme for the atmospheric contribute removal

3. DETECTION OF OBSTRUCTIONS

The obstructions represented in AOCs are elements (terrain, man-made objects, among others) geographically located over the earth surface, within the test area, presenting as a danger to the air-traffic. The detection of obstructions aims the safety and secure management of the air-traffic.
The DSM is a perfect data layer used to detect obstructions, because it represents the altitudes of the first reflective surface of the radar signal, i.e. top of the buildings, bridges, among other man-made objects.
The availability of several DSMs obtained during consecutive epochs of remote monitoring, provides the capability of detecting obstructions in each referred epoch.
Apart those several DSMs, another important data layer used to detect obstructions is the Obstruction Intersection Surface (OIS). This OIS is initially created in a vector format, expanding from the Airport Reference Point (ARP) outwards as defined in ICAO's annex 14 [5], and converted to a raster format in a latter step. In this OIS in raster format, every cell (the smallest element considered in the raster format, also named as *pixel*), has a Digital Number corresponding the maximum altitude where there should not exist any obstruction (also referred as objects that penetrate de OIS). An example of OIS is shown in fig. 5.

For the beginning of the process of obstructions detection, two raster layers (the same as a grid of cells) of the same test area are necessary, i.e. the DSM and the OIS (see fig.6). Meanwhile, it is important to refer that, whereas the DSM consists in a data layer that will be updated during consecutive epochs of remote monitoring, the OIS is generally static and does not change during those consecutive epochs, as long as the runway of the aeronautic infra-structure (an aerodrome) remains unchanged.

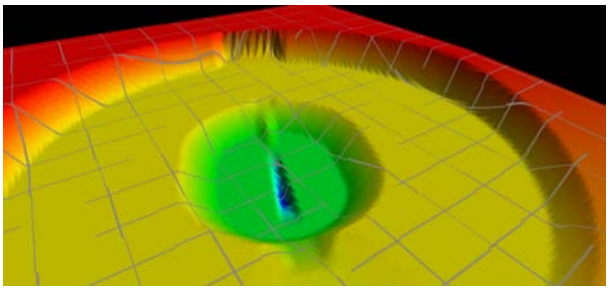

Figure 5. 3D representation of an OIS in raster format

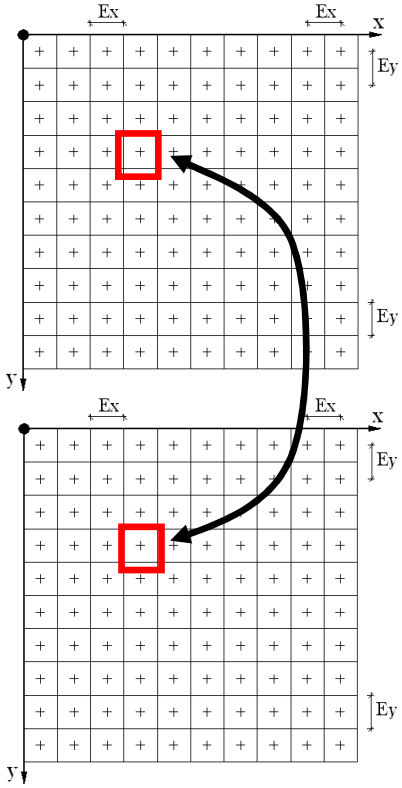

Figure 6. Overlay of DSM and OIS matrices (or grid of cells. The red square shows the analysis of a specific cell, positioned in 4th row and 4th line of the cell grid (or cell matrix). Ex and Ey concerns the horizontal and vertical resolution of the cell grid (or cell matrix), respectively.

Using the overlay function for the analysis of both DSM and OIS matrices, using the minus (-) operator, cells of the grid where altitude in DSM is greater than the altitude of the same cell in OIS it corresponds to an obstruction, while cells of the grid where altitude in DSM is lower than the altitude of the same cell in OIS corresponds to a transparent cell (i.e. no obstruction is detected).

The new surface obtained by the overlay (using the minus operator) of both DSM (the first data layer) and OIS (the second data layer) is also a surface in a raster format, designated as the Obstructions Surface (OS, the third data layer), where positive numerical value in each cell corresponds to those when DSM is higher than OIS, while a negative numerical value concerns the opposite case.

Since several Digital Surface Models are generated in consecutive epochs of remote monitoring, each DSM is labeled in accordance with the respective epoch. As an example, suppose the existence of a base DSM (the first DSM introduced into the system to detect obstructions, labeled T_0). Several consecutive DSMs in time are labeled as T_m, with $m = \{1,...,\infty\}$. For each pair of DSM and OIS, both labeled as T_m a respective OS is computed, again labeled as T_m, i.e.

$$OS_{T_m}(x,y) = DSM_{T_m}(x,y) - OIS_{T_m}(x,y) \quad (1)$$

where x and y are respectively the column and line indexes in the matrices.

The comparison of consecutive OSs in time is also made here, in accordance with

$$DifOS_k(x,y) = OS_{T_m}(x,y) - OS_{T_{m-1}}(x,y) \quad (2)$$

where *DifOS* is a differential obstruction surface, with $k = \{1,\ldots m\text{-}1\}$. Thus, according to the equation in (2), it is possible to evaluate or interpret the variance in altitude of obstacles, where:

a) a digital number greater than zero corresponds to a positive change, i.e. there is an increase in the height of the corresponding cell in the time frame T_m and T_{m-1};
b) a digital number smaller than zero corresponds to a negative change, i.e. there is a decrease in the height of the corresponding cell in the time frame T_m and T_{m-1};
c) a digital number equal to zero corresponds to no change, or that there is a static observation in the height of the corresponding cell in the time frame T_m and T_{m-1}.

Moreover, cells in a pair of consecutive Oss (ex: two OSs labeled T_m and T_{m-1}, where a positive difference was obtained and were considered as *no obstruction* and *obstruction* respectively in the OS labeled T_{m-1} and OS labeled T_m, are labeled as *new obstruction*. Cells in a pair of consecutive Oss (ex: two OSs labeled T_m and T_{m-1}, where a positive difference was obtained and were considered as *obstruction* and *no obstruction* respectively in the OS labeled T_{m-1} and OS labeled T_m, are labeled as *no longer obstruction*.

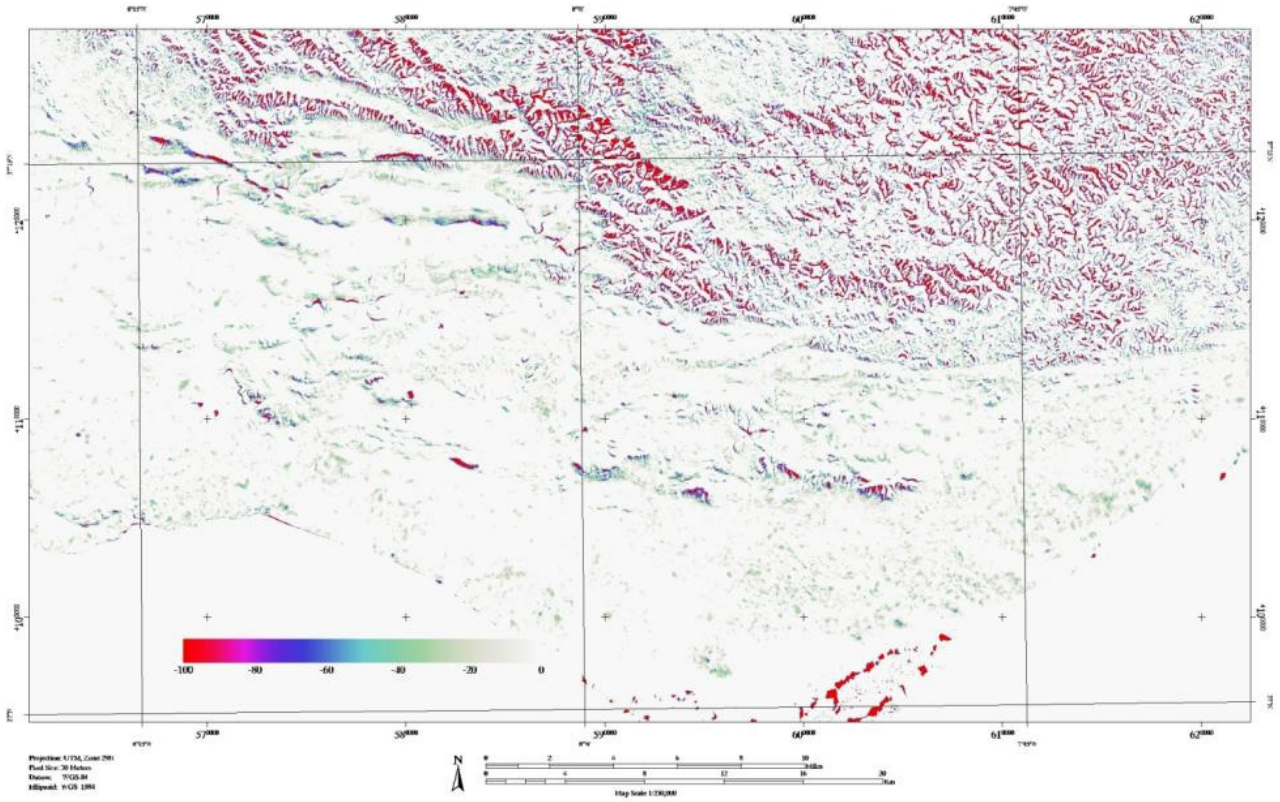

Figure 7. Difference map ($DifOS_k$) of Faro (white – no changes; purple to red – positive change).

Although we can represent all the three types of information in the same image, regarding the *absence* of change, *positive*, or *negative* change in height is DifOSs, in fact there is very little interest in *negative* changes in the height, unless they represented already a declared obstruction (or penetration) and in this case we already have substantial knowledge about it. Therefore, the color ramp proposed in Figure 7 should be scaled between a *no change* status, (within a certain threshold empirically chosen by the system operator after exhaustive testing) and *positive* change in height.

4. CONLUSIONS AND FUTURE WORK

The results obtained shows that the DSM produced with the SBAS technique presents the accordance with the numerical requirements stated in ICAO's annex 15, chapter 10 [5], with a vertical accuracy of about 30 meters for the test Faro, when compared with the raster ground truth obtained using digital photogrammetric. Although, the presences of slivers near shoreline with extremely lower frequency were found.

As future work, the usage of a special filtering procedure to eliminate the presence of slivers (outliers in DSM), usually located in the transition between the sea, or water bodies, to the ground area, will be taken into account. Additionally, the usage of binary matrices (*masks*) obtained when classifying the class *water* as '1' on land use layers of geospatial data and the remaining classes as '0' will be envisaged.

5. ACKNOWLEDGEMENTS

The authors acknowledge SARMAP and ITT Visual Information Solutions GmbH for the support and implementation of dedicated SARSCAPE module for ENVI [6] for high resolution DSM generation, and the Portuguese Army Geographic Institute (http://www.igeoe.pt) for the availability of the raster ground truth data used for validation purposes.

6. REFERENCES

[1] D. Damjanovic, "Using GIS and remote sensing to enhance air navigation safety", Photogrammetric and Engineering & Remote Sensing, ASPRS, May 2003, pp 478-481.

[2] A. Ferretti, C. Prati and F. Rocca, "Nonlinear subsidence rate estimation using permanent scatterers in differential SAR interferometry", Geoscience and Remote Sensing, IEEE Transactions on, vol. 38, no. 5, Part 1, Sept. 2000, pp. 2202 - 2212.

[3] Perissin, D.; Rocca, F.; , "High-Accuracy Urban DEM Using Permanent Scatterers," Geoscience and Remote Sensing, IEEE Transactions on , vol.44, no.11, pp.3338-3347, Nov. 2006.

[4] Berardino, P.; Fornaro, G.; Lanari, R.; Sansosti, E.; , "A new algorithm for surface deformation monitoring based on small baseline differential SAR interferograms," Geoscience and Remote Sensing, IEEE Transactions on , vol.40, no.11, pp. 2375- 2383, Nov 2002.

[5] http://www.icao.int

[6] http://www.ittvis.com/language/en-US/ProductsServices/ENVI/SARscape.aspx